nature communications

Article

https://doi.org/10.1038/s41467-025-60126-4

Expanded ribosomal synthesis of non-standard cyclic backbones in vitro

Received: 20 September 2024

Accepted: 13 May 2025

Published online: 28 May 2025

Check for updates

Kanghun Lee[1,5], Hyeongwoo Park[1,5], Ravi Kumar Devarapalli[2], Dahye Im[3], Jongcheol Seo[1,3] & Joongoo Lee[1,2,4]

The ribosome polymerizes *L*-α-amino acids into polypeptides, catalyzing peptide bond formation through aminolysis. This process is facilitated by entropy trapping within its peptidyl transferase center (PTC). In this research, we harness this capability to synthesize polymers containing cyclic motifs in the backbone. We design 26 non-canonical monomers (ncMs) with two distinct substrates: dicarboxylic esters and hydrazinoesters, each containing bifunctional moieties that undergo ring-closing reactions through multiple aminolysis reactions. Using a cell-free system that enables the consecutive incorporation of these ncMs into a growing peptide, we discover that the ribosome can produce 5- and 6-membered cyclic backbones, which have never been reported. We also demonstrate that the formation of such cyclic backbones within the ribosome is tunable by altering the substituents of dicarboxylic esters. This discovery expands the range of non-standard backbones that can be synthesized by the ribosome and motivates future research towards expanding ribosome-mediated chemistries for biopolymer synthesis.

The ribosome, an RNA-based catalyst, facilitates the formation of peptide (amide) bonds through a mechanism known as entropy trapping[1,2]. By positioning amino-acyl tRNA molecules in close proximity within a confined space, the ribosome reduces their conformational freedom, thereby enhancing the efficiency of peptide bond formation. This approach contrasts with typical catalytic strategies in synthetic chemistry, such as acid-base catalysis[3], and highlights the ribosome's ability to synthesize biopolymers (e.g., peptides or proteins). Uniquely, the ribosome, working in conjunction with other cellular machinery, can achieve sequence-defined, template-directed polymerization with high fidelity at speeds up to 17 monomers/second[4]. The core reaction, aminolysis, involves the nucleophilic α-amino group of an amino acid linked to the transfer RNA (tRNA) at the ribosome's A-site attacking the electrophilic carbonyl carbon in the ester linkage of the tRNA in the ribosome's P-site (Fig. 1)[5,6]. Despite an evolutionary preference for a set of 20 canonical amino acids, the ribosome can also polymerize a wide array of non-canonical monomers (ncMs) through aminolysis, resulting in the formation of amide backbone. These ncMs vary significantly in size, shape, and chemical characteristics, including a diverse range: α-, β-, γ-, δ-, ε-, ζ-, D-amino acids and non-amino carboxylic acids[7–17]. Incorporating ncMs into proteins broadens the spectrum of chemical diversity and functionality of biopolymers. This development holds promise for producing enzymes and therapeutics with enhanced or distinct properties[18–28].

Building on previous efforts to expand the range of substrates, the field has advanced in developing peptide isosteres by leveraging the ribosome's capability for synthesizing linear polypeptides. The replacement of amino acids with structural analogs such as hydroxy-, thio-, and aminocarbothio-acid has demonstrated that the ribosome can directly produce polyesters, polythioesters, and polythioamides, respectively[17,29–31]. Another significant advancement that challenges the natural functions of the ribosome is the introduction of cyclic

[1]Division of Interdisciplinary Bioscience and Bioengineering (I-Bio), Pohang University of Science and Technology (POSTECH), Pohang 37673, Republic of Korea. [2]Department of Chemical Engineering, Pohang University of Science and Technology (POSTECH), Pohang 37673, Republic of Korea. [3]Department of Chemistry, Pohang University of Science and Technology (POSTECH), Pohang 37673, Republic of Korea. [4]Institute for Convergence Research and Education in Advanced Technology, Yonsei University, Seoul 03722, Republic of Korea. [5]These authors contributed equally: Kanghun Lee, Hyeongwoo Park.
e-mail: jgoolee@postech.ac.kr

https://doi.org/10.1038/s41467-025-60126-4

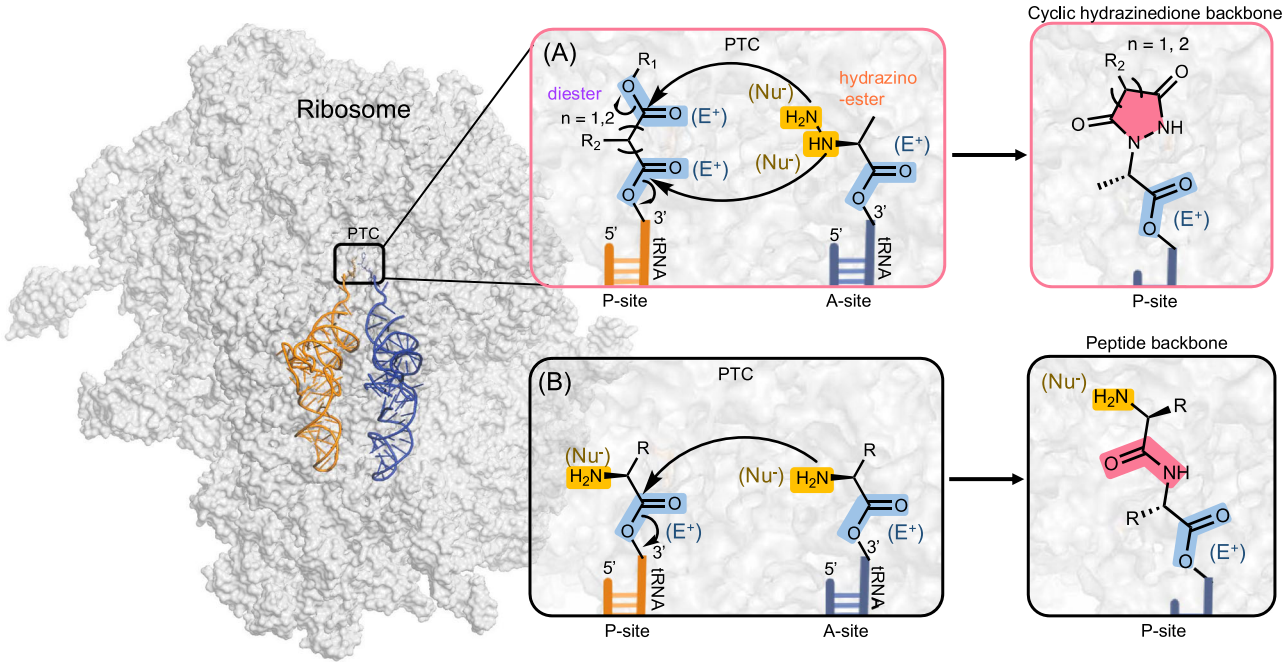

Fig. 1 | Formation of cyclic hydrazinedione bonds within the ribosome. The structure of the ribosome (gray) and tRNAs (orange and blue) involved in bond formation from previously published work (PDB ID: 1vy4). **A** Bifunctional substrates containing two electrophiles (E^+) and nucleophiles (Nu^-) engage in ring-closing reactions via successive aminolysis within the ribosome, resulting in the formation of cyclic structure. **B** The typical ribosome-mediated peptide bond formation mechanism involving a nucleophilic substitution reaction (See Supplementary Fig. 2 for further details on the proposed mechanism).

backbones into peptides. These cyclic motifs are important for peptide-based natural products as they enhance proteolytic resistance, structural rigidity, and specificity towards target proteins[32,33], often resulting in increased drug efficacy. Such examples include penicillin V (dipeptide of Cys-Val), goadsporin (polyazole antibiotics), and patellamide C (macrocyclic antimicrobial peptides) (Supplementary Fig. 1). The production of these cyclic structures in peptides was initially sought using indirect methods, where the peptide is first synthesized using a ribosome to contain amino acids with reactive side chains toward enzymatic reactions, followed by an enzymatic ring-closing reaction. Examples of enzymes involved in these reactions include PatD, GodD, and LazDE, cyclohydratases that form heterocyclic azoline derivatives using Cys, Ser, or Thr[34,35]. More recently, a direct method for cyclic motif production was developed, where ncMs are attached to tRNA using a genetic code reprogramming approach, and ribosomes facilitate a cyclocondensation reaction between the two sequentially incorporated ncMs in vitro[17]. This finding demonstrates the ribosome's ability to catalyze ring-closure reactions. Despite the advancement, the full scope of reactions that ribosomes can catalyze remains largely unexplored. Expanding the diversity of cyclic backbones could deepen our understanding of ribosomal polymerization and widen the array of precisely tailored motifs within polypeptides particularly relevant in pharmaceutical applications.

In this study, we aim to demonstrate the ribosome's ability to directly synthesize diverse cyclic structures, thereby expanding the chemical space for abiological polymers. To achieve this, (i) we design two classes of bifunctional substrates, each containing two electrophiles and nucleophiles; in the peptidyl-transferase center (PTC), these substrates undergo ring-closing reactions to form cyclic backbones rather than a peptide bond (Fig. 1). (ii) Next, by adjusting the spacing and geometry of those reactive handles, we generate diverse 5- and 6-membered rings (Fig. 2). (iii) Furthermore, cyclization efficiency is modulated by systemically altering the kinetic properties of the substrates substituents (Figs. 3 and 4), allowing the rate and yield of ring formation to be tuned. (iv) We then show that minimal RNA constructs mimicking the ribosomal active site catalyze the same formation reaction, suggesting that RNA alone can assemble these non-canonical backbones (Figs. 5 and 6). (v) Finally, we present evidence that cyclization occurs at defined positions on the substrate, consistent with the wild-type ribosome's evolved preference for α-amino acids over those with other non-canonical amino acids bearing an extended carbon chain (e.g., β-amino acids) (Figs. 1 and 7). Collectively, this study demonstrates that the ribosome and its RNA core can directly synthesize a variety of 5- and 6-membered cyclic structures, deepening our understanding of the ribosome's bond-forming mechanism.

Results

Synthesis of ncMs-acylated tRNAs for ribosome-mediated polymerization in vitro

The synthesis of cyclic backbones using the ribosome requires ncM-acylated tRNAs (Fig. 2). The conventional approach to charging ncMs onto tRNAs involves engineering aminoacyl-tRNA synthetases (aaRSs), the enzymes responsible for attaching natural amino acids to their corresponding tRNAs. However, engineered aaRSs have limited promiscuity and can only accommodate a narrow range of amino acids structurally similar to those used in the engineering process[36]. To overcome this limitation, we employed the aminoacylating ribozyme, flexizyme (Fx), which catalyzes tRNA acylation by recognizing an aromatic group[37] of an activated ester substrate. Fx has demonstrated extensive compatibility with a diverse range of ncMs with aromatic rings[10,12,38], thus expanding the scope of ribosome-mediated synthesis of emerging bio-based materials[39]. Currently, four different ester or thioester leaving groups (flexizyme leaving group (FLG), Fig. 2A) are used in conjunction with three flexizyme variants (eFx, dFx, and aFx): eFx/cyanomethyl ester (CME), dFx/dinitrobenzyl ester (DNB) or chlorobenzyl thioester (CBT), and aFx/(2-aminoethyl)amidocarboxybenzyl thioester (ABT). The selection of the appropriate Fx and corresponding FLG depends on the physicochemical characteristics of the substrate[40]. For example, substrates bearing an aromatic group within their structure (e.g., phenylalanine) are optimally suited for CME. In contrast, substrates lacking an aromatic residue (e.g., lysine) require DNB or CBT, while hydrophobic substrates (e.g., leucine) are best

https://doi.org/10.1038/s41467-025-60126-4

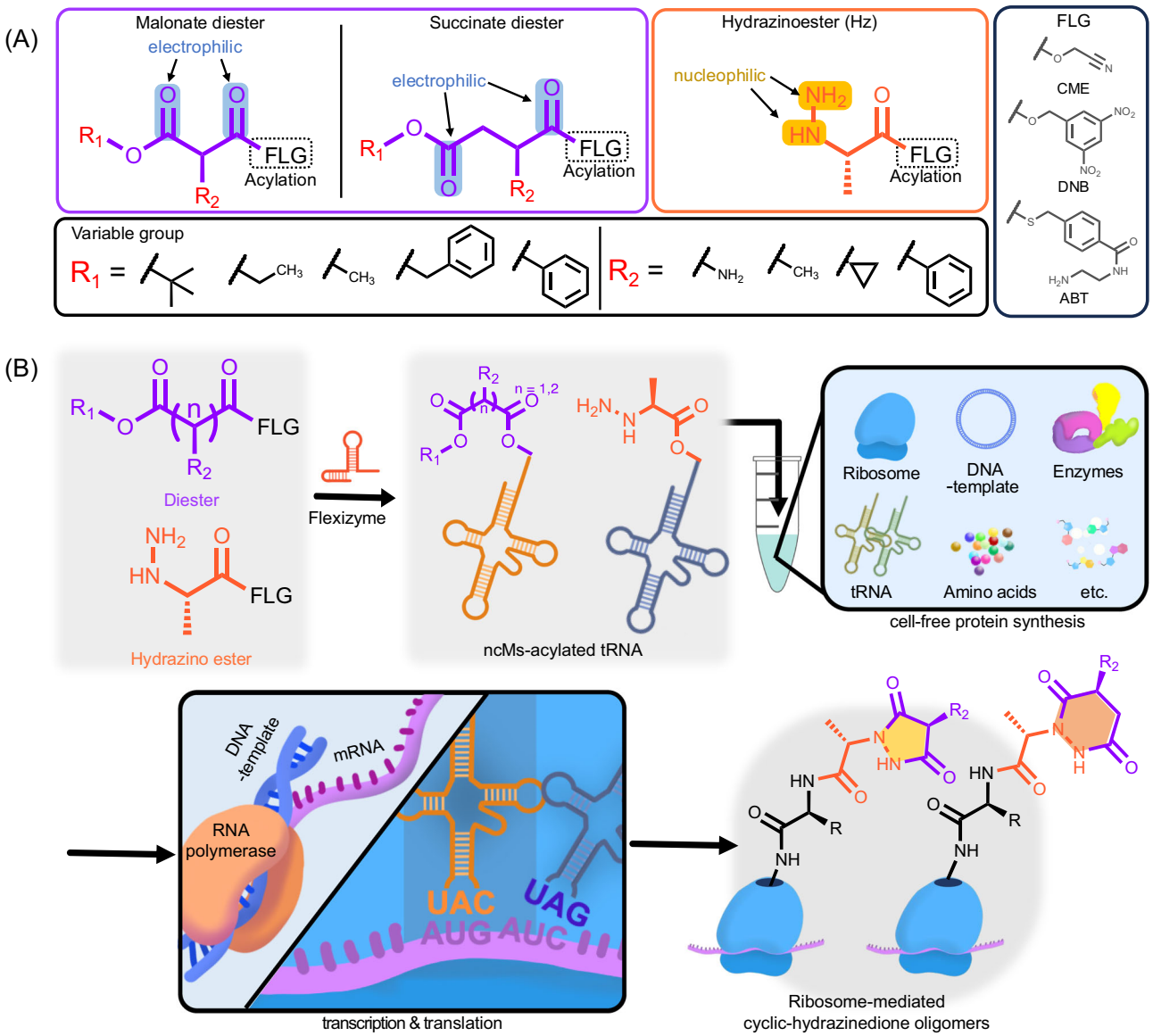

Fig. 2 | Substrate design principle and genetic code reprogramming for producing cyclic structures in a cell-free system. A Each substrate was activated with a flexizyme leaving group (FLG), an essential motif for recognition by flexizyme (Fx). The diester substrates were synthesized from malonic and succinic acid, each containing two electrophiles but differing in the number of carbon atoms in their structure. The substrates were further diversified by varying the R_1 and R_2 substituents. As synthons, we designed a hydrazinoester containing two nucleophilic nitrogen atoms. **B** Fx was used to acylate the substrate onto in vitro transcribed synthetic tRNAs. Following the flexizyme-mediated acylation of diester (violet) and hydrazinoester (orange), each acylated tRNA:ncM complex was added to a cell-free protein synthesis platform to decode two consecutive codons programmed on mRNA. The ribosome then forms non-standard 5- and 6-membered rings while polymerizing the two monomers, demonstrating its potential as a versatile chemical apparatus capable of facilitating previously unachieved synthetic reactions.

matched to ABT due to the water-solubilizing moiety (-NH_3^+) on the aromatic component[38]. The recently reported 'Fx substrate design rules' have more broadened the scope of Fx applications by providing guidelines for identifying ncMs compatible with Fx-mediated acylation[37].

Design of chemical substrates for ribosome-mediated cyclic bond formation

Diesters and hydrazines have been used as substrates to produce heterocyclic structures, where the diester serves as a scaffold for the cyclic structure and react with the hydrazine via a nucleophilic substitution reaction at the two reactive groups. This reaction, however, typically requires high temperatures and a catalyst (acid or base)[41,42], along with an excess of one of the reactants. Utilizing the ribosome as a catalyst for synthesizing this motif would provide a distinct platform, enabling rapid synthesis in an aqueous solution under moderate temperatures (30–37 °C) as well as taking advantage of the ribosome's template-guided sequence-specific polymerization capability[43]. To design a diester substrate compatible with Fx, we first converted an acid moiety to an ester containing an FLG (Fig. 2A). We next derivatized the other acid with different R_1 substituents that vary the steric hindrance and electron density around the electrophilic carbonyl carbon. R_1 substituents include *tert*-butyl, ethyl, methyl, benzyl, and phenyl groups. The choice of R_1 may allow the rate of the cyclization reaction to be finely controlled[44,45]. We also varied substituent R_2 (Fig. 2A) with aliphatic, branched-chain, and aromatic variants, demonstrating that ribosome-mediated synthesis can produce a diverse array of heterocyclic derivatives more efficiently than the conventional solution-based chemistry. Furthermore, we varied the carbon chain length (malonate; 3-carbon chain, and succinate; 4-carbon chain), which produces different ring sizes once cyclization occurs (Fig. 2B). As a synthon for forming cyclic

https://doi.org/10.1038/s41467-025-60126-4

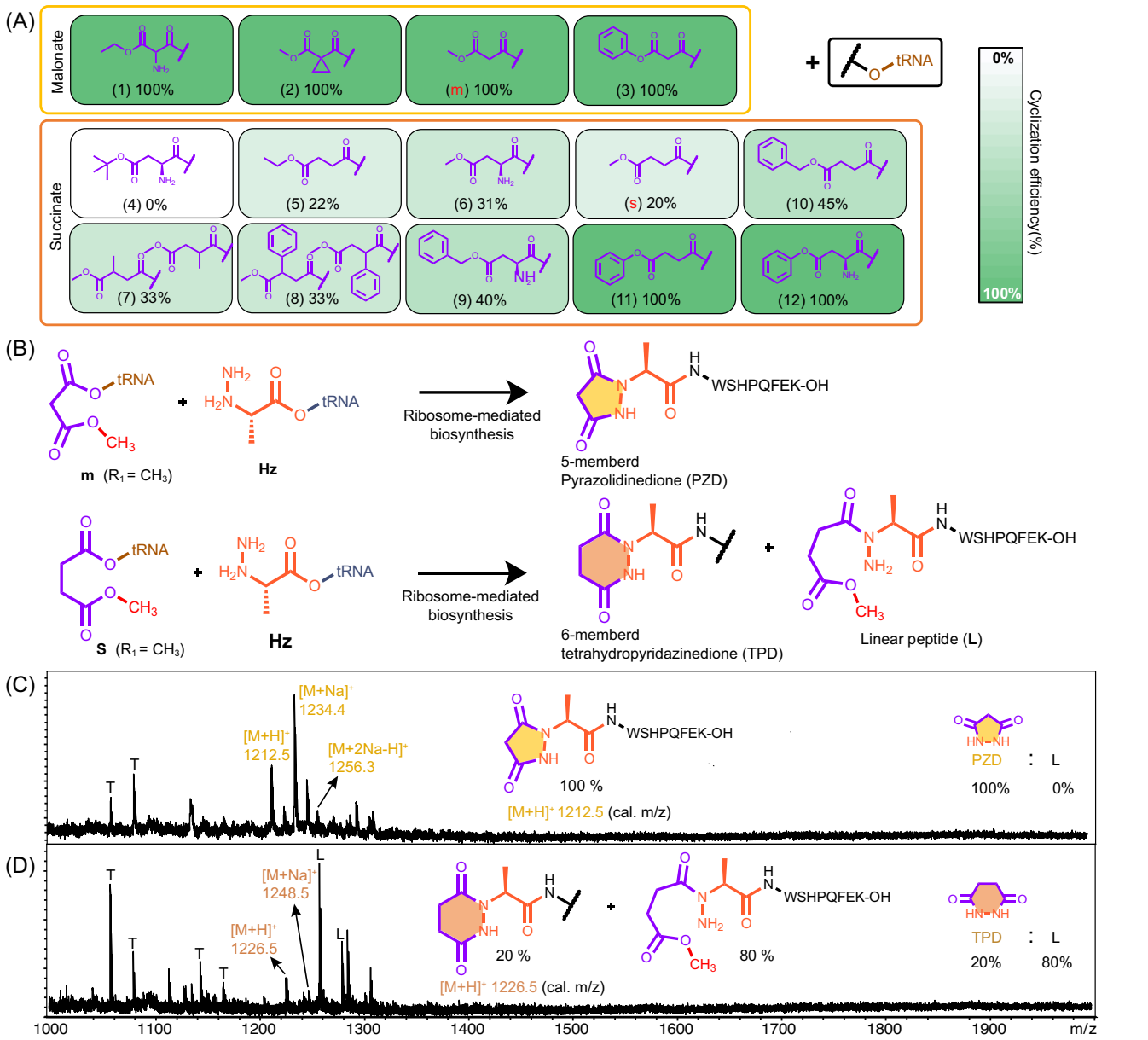

Fig. 3 | Expanding the substrate palette for 5- and 6-membered ring formation. **A** The diester substrates were systemically designed based on the structure of malonic and succinic acid. Out of 21 malonate and succinate derivatives (Supplementary Fig. 3), 14 synthetic diester substrates (**1**–**12**, **m**, **s**) were successfully charged to tRNA by Fx, resulting in an ncM:tRNA^{fMet} (CAU) conjugate. Similarly, **Hz** was charged to tRNA by Fx, yielding **Hz**:tRNA^{ProIE2} (GAU). Cyclization efficiency, measured as the ratio of peak intensities representing peptides with cyclic structures relative to linear peptide oligomers is depicted with shade intensity according to a color map. **B** Upon introducing **m**:tRNA^{fMet} (CAU) and **s**:tRNA^{fMet} (CAU) with **Hz**:tRNA^{ProIE2} (GAU) into PURExpress™ (NEB) system, the ribosome successfully synthesizes 5- and 6-membered ring structures, respectively. **C** Mass spectrometric analysis of the reaction between substrates **m** and **Hz** within the ribosome produced a high yield (100 %) of peptide oligomer with a cyclic pyrazolidinedione group at the N-terminus. **D** However, the reaction between substrate **s**, which bears the same R_1 substituent, and **Hz** yielded only 20 % cyclic structure alongside 80 % linear product, indicating incomplete cyclization. Note that substrates **7**–**8** were synthesized as a mixture (see Supplementary Fig. 10) and were used as such. The production of N-terminus truncated peptide (denoted as T) is often observed in prokaryotic cell-free protein synthesis[74,75]. This truncation occurs due to the inefficiency of the synthetic tRNAs with ncM (**s**:tRNA^{fMet} and **Hz**:tRNA^{ProIE2}) in forming the translation initiation complex, leading to premature 'drop-off' the initiator tRNA before peptide synthesis is completed. Consequently, the ribosome reinitiates translation at a downstream codon using endogenous tRNAs with natural amino acids[76,77]. Spectra in (**C**, **D**) are representative of $n = 3$ independent experiments. Source data are provided as a Source Data file.

structures, we employed 2-hydrazinylpropanoic acid; **Hz**, (Fig. 2A)[17], which also exhibits bifunctional nature due to its two nucleophilic nitrogen atoms (Supplementary Fig. 3).

Fx-mediated acylation of ncMs and ribosome-mediated synthesis of cyclic motifs

We conducted Fx-mediated reaction in two stages to charge ncMs onto tRNAs. Initially, we used a short microhelix tRNA (mihx), a 22-nucleotide tRNA analog, to determine the optimal conditions for acylation. This method offers rapid analysis because acylated mihx, with its increased molecular weight, can be distinguished from unacylated mihx due to their differing mobility on a polyacrylamide gel (Supplementary Figs. 4–6). For each ncM, six different experimental conditions were tested, varying pH levels (7.5 and 8.8) and Fx variants (eFx, dFx, and aFx) to identify the condition with the highest acylation yield[16]. We quantitatively assessed the acylation yield through densitometric analysis of

https://doi.org/10.1038/s41467-025-60126-4

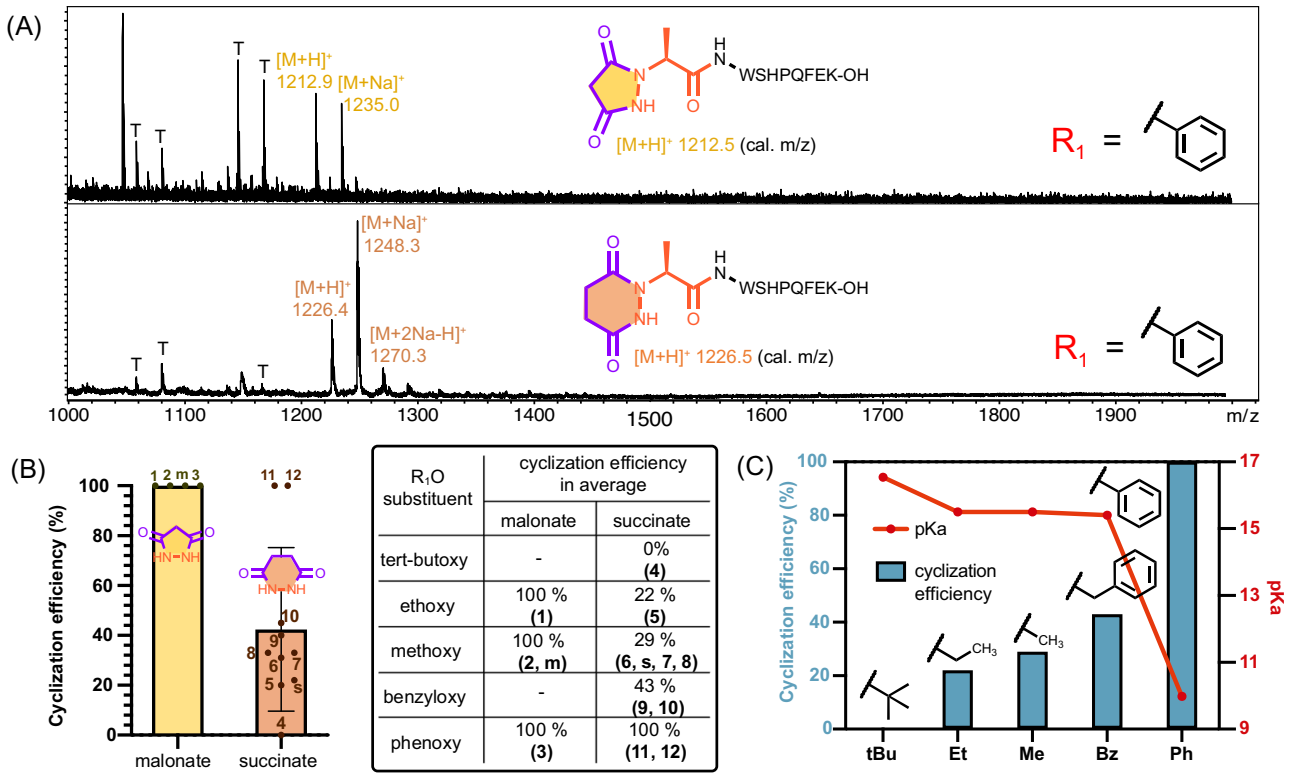

R_1O substituent	cyclization efficiency in average	
	malonate	succinate
tert-butoxy	-	0% **(4)**
ethoxy	100 % **(1)**	22 % **(5)**
methoxy	100 % **(2, m)**	29 % **(6, s, 7, 8)**
benzyloxy	-	43 % **(9, 10)**
phenoxy	100 % **(3)**	100 % **(11, 12)**

Fig. 4 | Effect of R_1 substituents on cyclization efficiency (ratio of cyclic to linear product). A Substrates **3** and **11** bearing a phenyl substituent for R_1 were tested for cyclization. For malonate diester substrates, cyclization to form 5-membered rings was nearly complete (~100 % efficiency), indicating that the nature of R_1 has minimal influence on this process due to rapid ring-closure kinetics (upper panel). A notable enhancement in the formation of 6-membered rings was observed when R_1 was altered from methyl to phenyl, with no detectable linear peptide byproduct (lower panel). Spectra in (**A**) are representative of $n = 3$ independent experiments. **B** The cyclization efficiency of the 6-membered ring for succinate diester is considerably lower than that of 5-membered ring for malonate diester, when the R_1O^- substituent is ethoxylate (substrate **5**) and methoxylate group (substrates **6**, **s**, **7**, and **8**, see the table). The formation of 5-membered rings within the ribosome is kinetically most favorable, while the synthesis of 6-membered rings presents a challenge. Each cyclization efficiency value is the average of $n = 3$ independent experiments. **C** The challenge of 6-membered ring formation is lowered by the chemical properties of R_1O^- substituents. Phenoxylate with lower basicity (pKa of ~10) enhances cyclization efficiency during the aminolysis reaction. Source data are provided as a Source Data file.

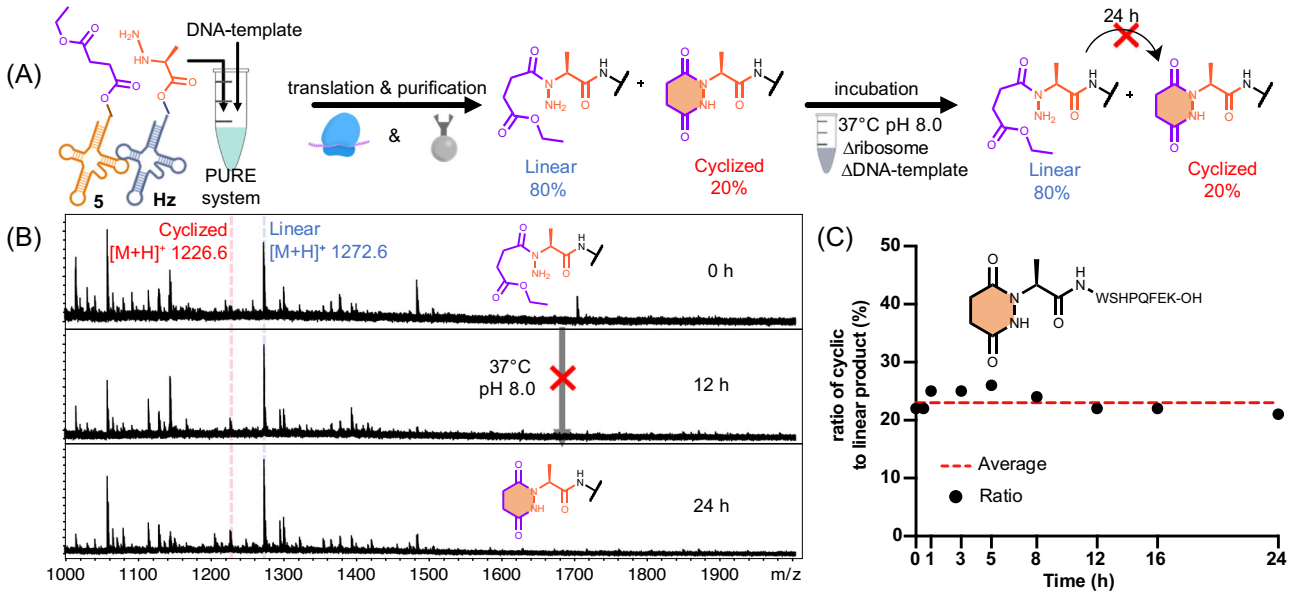

Fig. 5 | No cyclization reaction occurs through self-cyclization in solution. A–C The constant peak intensity of the linear product over time indicates that the cyclic products are not generated by a simple self-cyclization reaction. (See Supplementary Fig. 16 for all the mass spectra obtained at the given time points). Spectra in (**B**) are representative of $n = 3$ independent experiments. Source data are provided as a Source Data file.

https://doi.org/10.1038/s41467-025-60126-4

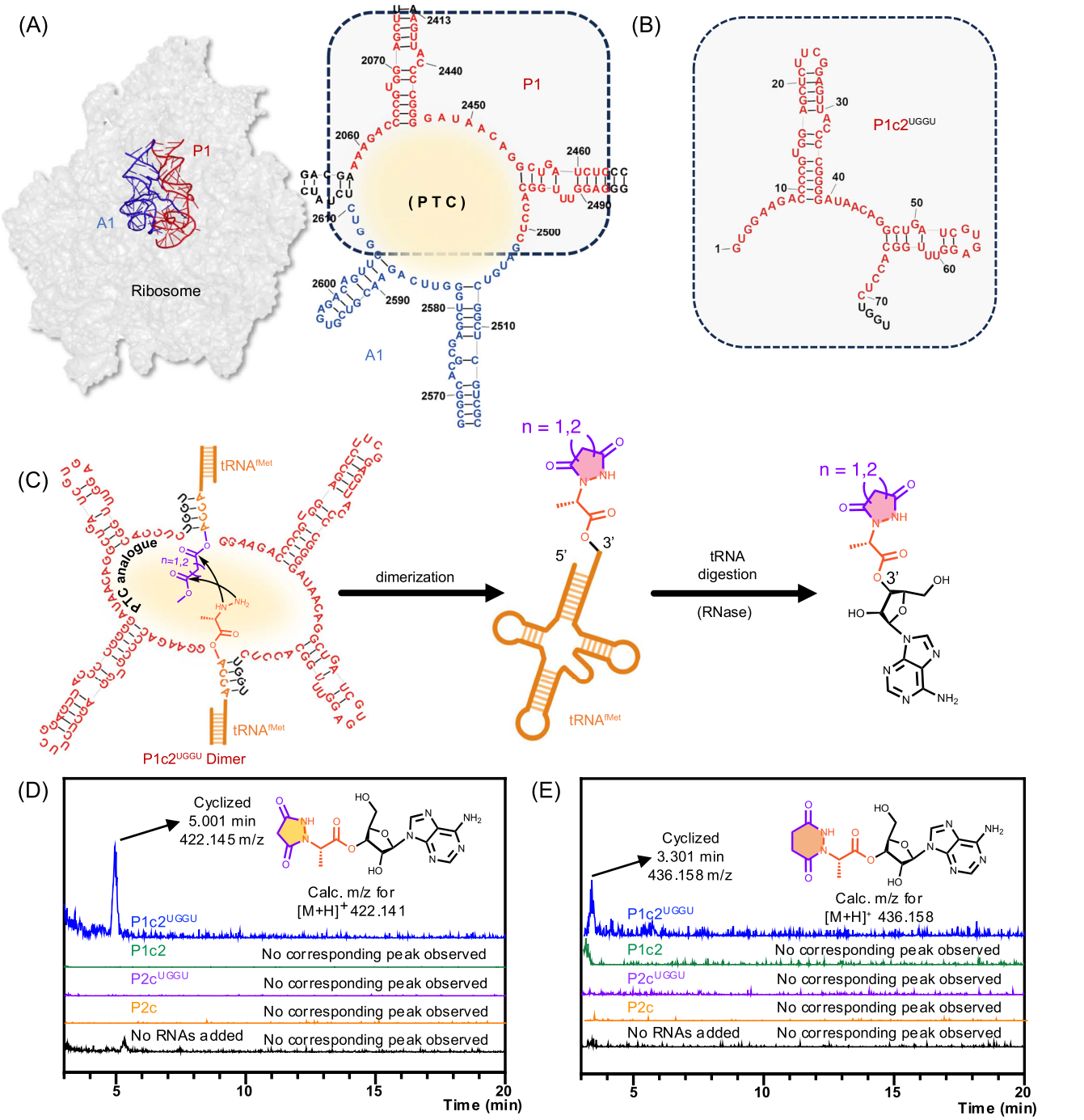

Fig. 6 | Cyclization in analogues of the peptidyl transferase center. A The P1c2^{UGGU} domain, which partially includes the ribosome's catalytic domain (domain V), was prepared via in vitro transcription. **B** P1c2^{UGGU} was designed with a UGGU sequence to enable base-pairing with a tRNA bearing an ACCA sequence at its 3′-end, thereby positioning the substrates in close proximity and facilitating catalytic activity comparable to that of the full ribosome. **C** Upon dimerization, the P1c2^{UGGU} domain forms a catalytic pocket akin to the peptidyl transferase center. This arrangement allows the two tRNA-charged substrates to undergo cyclization. Subsequently, RNase digestion of the resulting tRNAs yields the expected product attached to the 3′-end residue of the tRNA. **D**, **E** The extracted ion chromatograms show a single peak corresponding to the theoretical mass of a 5- and 6-membered ring linked to the 3′-OH of adenosine, only in the presence of catalytically functional P1c2^{UGGU} in the solution (blue, $[M+H]^+$ = 422.141 (cal), $[M+H]^+$ = 422.145 (obs) for 5-membered ring and $[M+H]^+$ = 436.158 (cal), $[M+H]^+$ = 436.158 (obs) for 6-membered ring). P1c2, lacking the interaction of tRNA due to the elimination of the UGGU sequence, does not exhibit the ability to catalyze peptide bond formation (green). Similarly, reactions with P2c^{UGGU}, of which structure is mutated to be inactive, produce no cyclic products (purple), suggesting that simple proximity is insufficient for cyclic structure formation. Additionally, reactions with P2c (orange), which lacks both catalytic activity and tRNA interaction, yield no corresponding products. No corresponding products were observed in the absence of PTC analogues (black). Spectra in **D** and **E** are representative of n = 3 independent experiments. Source data are provided as a Source Data file.

https://doi.org/10.1038/s41467-025-60126-4

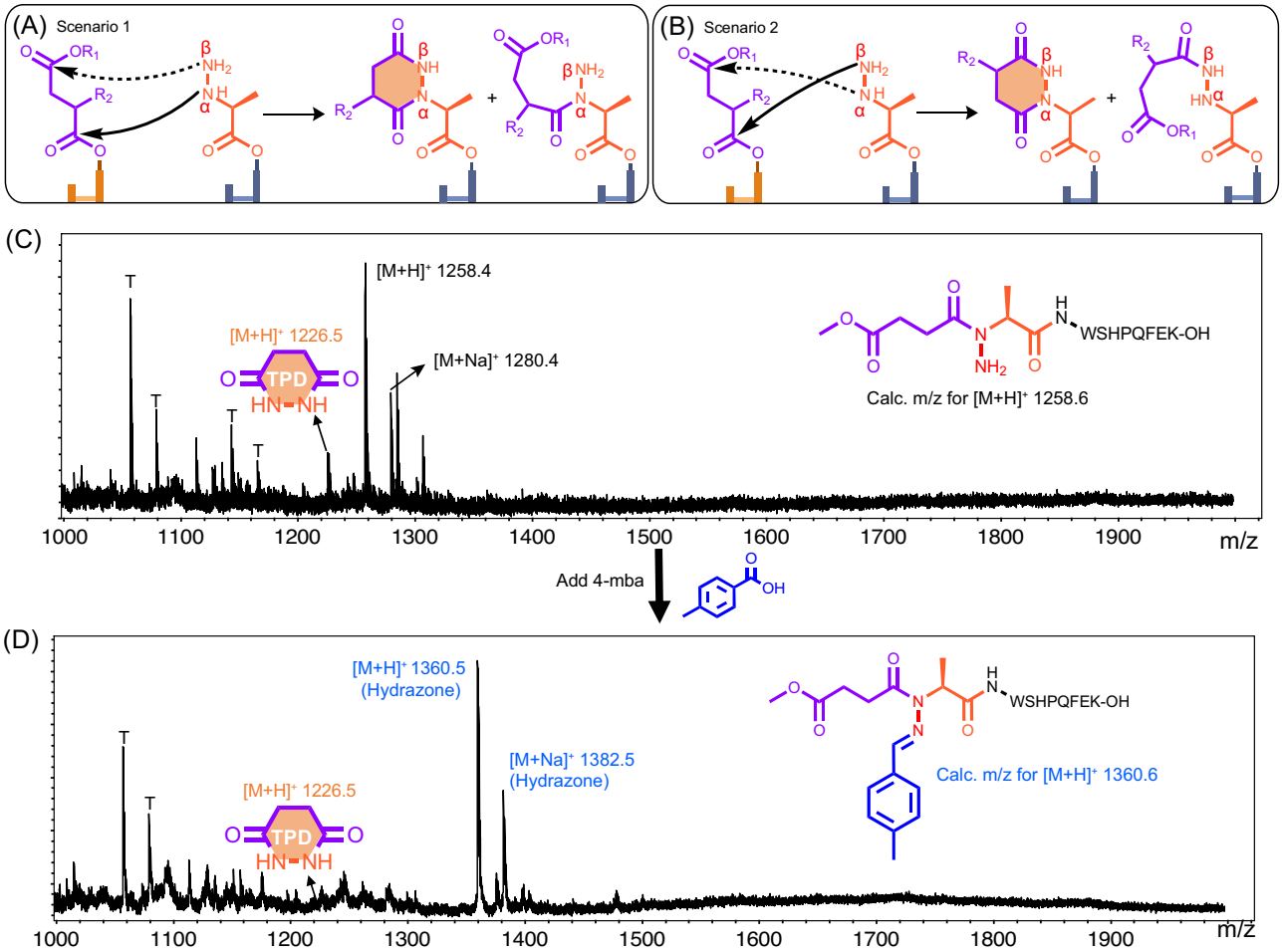

Fig. 7 | Two potential mechanisms are proposed for the cyclization process within the ribosome. A In the first scenario, the α-nitrogen atom of **Hz** initiates an attack on the tRNA ester linkage, while the β-nitrogen atom targets the R_1 ester linkage, facilitating ring closure. **B** The second scenario proposes the reverse order of attacks, leading to the formation of a regioisomeric cyclic structure. **C**, **D** The reaction of the resulting linear peptide with 4-mba, a reagent that specifically reacts with free primary amines, showed a single peak ($[M+H]^+$ = 1360.5) corresponding to the mass of the linear product of a hydrazone. This is direct evidence that a free primary amine is present within the peptide, suggesting that the α-nitrogen was used to form the peptide bond and the β-nitrogen was used for ring-closure. Spectra in C and D are representative of n = 3 independent experiments.

gel bands. Once optimal conditions are identified, we acylate a full-length tRNA molecule with the respective ncM.

We first charged substrate **m** (a malonic ester derivative) and **Hz** to microhelix (Fig. 3A and Supplementary Fig. 3). Substrate **Hz** achieved over 50 % acylation, whereas substrate **m** did not show any significant band shift on the polyacrylamide gel. This lack of shift is presumably due to the faster electrophoretic mobility of substrate **m** in the acidic gel (pH 5.2), which is attributed to the absence of a positively charged moiety (e.g., $-NH_3^+$) (Supplementary Fig. 4). Acylation of substrate **m** to tRNA by Fx is essential for achieving ribosome-mediated biosynthesis of non-native chemical bonds through two consecutive incorporations of both substrates. Thus, we sought to measure successful acylation of substrate **m** to tRNA through more sensitive means. To achieve this, we performed a Fx-mediated acylation reaction with substrate **m** to $tRNA^{fMet}$ (CAU). For ribosome-mediated biosynthesis, we purified the acylated tRNA through ethanol precipitation to remove any unreacted substrate **m**. The resulting **m**:$tRNA^{fMet}$ (CAU) conjugate was then re-suspended in an aqueous buffer and introduced into PURExpress™ (NEB), a reconstituted in vitro protein synthesis system. To facilitate the analysis of the products, we designed a reporter gene producing a Strep tag (XWSHPQFEKST) on a T7 promoter-controlled DNA plasmid (pJL1_X-StrepII-ST), where X indicates the position to which Fx-charged **m** is incorporated. We selected the Strep tag due to its high affinity for Strep-Tactin and the ability to elute target peptides under mild denaturing conditions (0.1 % SDS)[46]. The reaction was carried out at 37 °C for 2 h in the presence of the other eight amino acids required for synthesis of the peptide containing a Strep tag. The reaction products were purified, eluted, and subsequently characterized via MALDI-TOF mass spectrometry. The mass spectrum analysis identified a peak corresponding to the theoretical mass ($[M+H]^+$ = 1346.6; $[M+Na]^+$ = 1368.8) of the product containing **m** at the N-terminus (Supplementary Fig. 7C), confirming substrate **m** is charged to tRNA by Fx. The acylation yield is estimated to be over 50 % based on our previous study[17], which analyzed the relationship between the acylation and translation yield using peak intensities from the MALDI spectrum (Supplementary Fig. 8).

For substrate **Hz**, we carried out Fx-mediated reaction for $tRNA^{Pro1E2}$ (GAU) using the same method. An engineered proline-tRNA was chosen for its efficient incorporation of ncMs into peptides in previous studies[11,47,48]. The resulting **Hz**:$tRNA^{Pro1E2}$ (GAU) conjugate was introduced to a PURExpress reaction containing **m**:$tRNA^{fMet}$ (CAU) and a DNA plasmid (pJL1_XY-StrepII). This DNA template encodes a Strep tag (XZWSHPQFEK), containing the two ncMs at positions X and Z (Fig. 3B). The Met(AUG) and Ile(AUC) codons were selected for X and Z, because Met and Ile are not required for Strep

tag synthesis (and hence avoid competition with natural amino acids), and AUG is necessary as the initiation codon in protein synthesis. The resulting peptide was characterized using MALDI-TOF mass spectrometry, showing a peak corresponding to the theoretical mass ($[M + H]^+ = 1212.5$; $[M+Na]^+ = 1234.4$; $[M + 2Na\text{-}H]^+ = 1256.3$) of the product containing a pyrazolidinedione at the N-terminal region (Fig. 3C and Supplementary Fig. 9). To the best of our knowledge, this study provides evidence that the ribosome can catalyze the synthesis of a 5-membered cyclic structure.

Exploring further, we next tested ribosomal synthesis utilizing a wide spectrum of monomers containing diverse non-canonical backbones for incorporation into a growing polymer by the ribosome (Fig. 3A). We focused on diesters containing an extended carbon chain capable of forming larger cyclic structures through the ring-closure mechanism with substrate **Hz** inside the ribosome (Fig. 3B). For this, we chose succinic ester and designed a derivative (**s**) to have the same R_1 substituent. We then found an optimal acylation condition (pH 8.8 and aFx) for tRNA charging by carrying out the Fx/mihx experiments and mass spectrometric analysis (Supplementary Fig. 5 and 7G). With Fx-charged **s**:$tRNA^{fMet}$ (CAU) with **Hz**:$tRNA^{Pro1E2}$ (GAU), we carried out in vitro translation using PURExpress™ and characterized the resulting product using mass spectrometry. The MALDI spectrum showed a peak corresponding to the theoretical mass of the peptide containing a 6-membered tetrahydropyridazinedione at the N-terminus ($[M + H]^+ = 1226.5$; $[M+Na]^+ = 1248.5$, Fig. 3D). Although a previous study reported the 6-membered structure with a pyridazinone ($C_4H_6N_2O$) motif produced by the ribosome[17], our study has discovered a distinct cyclic structure with the pyrazolidinedione motif ($C_4H_6N_2O_2$).

Intriguingly, the mass spectrum (Fig. 3D) showed major peaks that did not correspond to the expected mass of product containing the 6-membered structure. The mass analysis suggests that the major peak (denoted as T) corresponds to the theoretical mass of a truncated peptide without any synthetic substrates at the N-terminus. However, the peak L matched the peptide containing substrate **s**, with a peptide bond connected to a single nitrogen atom from substrate **Hz** (Fig. 3B).

We also considered the scenario in which the appropriate substrates are incorporated into the peptide, but the ring closing reaction is not efficiently carried out, resulting in a linear product (Fig. 3B). To determine the ratio of cyclic to linear products, we calculated the percentage based on peak areas, assuming a calibration factor of 1.0 (Supplementary Fig. 11) as observed in our previous study[17]. Based on this calculation, we found that only 20 % of the cyclic product was produced from substrate **s** (Fig. 3D), while the reaction with substrate **m** yielded no linear product (Fig. 3C), indicating nearly 100 % cyclization efficiency. We hypothesized that this is due to the fast kinetics of 5-membered ring formation, attributed to reduced ring strain and a stable transition state, as observed in solution chemistry[49,50]. To test this hypothesis further, we looked to experiments that allowed us to tune the kinetic rate of ring formation.

Mechanistically, the formation of cyclic structure between a diester and a hydrazinoester, two sequential aminolysis reactions must occur within the ribosome. This involves release of both tRNA and alkoxide (R_1O^-) from the two carbonyls of diester substrates. In the two reactions using substrates **m** and **s**, methoxide (CH_3O^-), a conjugate base of methanol, with high basicity (pKa of ~16) is expelled as a leaving group. We hypothesized that high basicity makes methoxide less prone to dissociate and that altering the R_1 substituent to groups with different pKa may affect the kinetics of ring-closure reaction. To test this hypothesis, we designed malonate and succinate derivatives with various R_1 groups (*tert*-butyl, ethyl, benzyl and phenyl) and various pKas (Figs. 2A and 3A).

The cyclization kinetics are influenced by the R_1 substituents

First, we synthesized a range of malonic ester derivatives (substrates **1**–**3**), varying the R_1 group (ethyl (**1**), methyl (**2**), and phenyl (**3**)) to evaluate their impact on forming 5-membered rings (Fig. 3A). We also varied R_2 groups (R_2 = H, amino, and cyclopropyl) (Supplementary Fig. 12) to test if the ribosome's potential to catalyze the synthesis of 5-membered pyrazolidinedione derivatives is independent of an additional functional group attached to the carbon chain. After Fx-mediated tRNA acylation reaction and subsequent ribosomal synthesis with **Hz**:tRNA in the PURExpress system, we characterized the resulting products by MALDI mass spectrometry. In the MALDI spectrum (Fig. 4A (upper panel) and Supplementary Fig. 9), a peak corresponding to the peptide containing the desired 5-membered ring structure was observed. Notably, peaks indicative of the linear form were absent across the different R_2 substituents (i.e. substrates **1**, **2**, and **3**). This suggests that the basicity of the R_1 substituent, which ranges across seven orders of magnitude in pKa (from phenolate to ethoxylate), and the bulkiness of the R_2 substituent have minimal impact on the efficiency of 5-membered ring formation within the ribosome. This is presumably because the rapid kinetics of ring formation minimizes the potential impact of substituents.

We next examined the impact of R_1 substituents on the formation of 6-membered rings. To explore this, we used nine succinic ester derivatives (substrates **4**–**12**) with different R_1 groups (Fig. 3A). Notably, substrate **4** containing a *tert*-butyl substituent yielded no cyclized product (cyclization efficiency: 0 %, Fig. 3A and Supplementary Fig. 10). We hypothesized that this was due to the following two key factors: (i) the *tert*-butyl group creates significant steric hindrance, which impedes nucleophilic attack on the carbonyl carbon, a rate-determining step in aminolysis, and (ii) the *tert*-butoxylate has a higher basicity (pKa ~17) and thus is less favorably displaced from the carbonyl carbon compared to substrate **s** containing a methoxy substituent (Figs. 3A and 4B). In this context, a less bulky or less basic substituent may improve the cyclization efficiency. To test this hypothesis, we designed substrates **5**-**8** with ethyl or methyl groups (pKa ~16). These products showed an increased cyclization efficiency of ~30 ± 5 % in the formation of 6-membered ring. Substrates **9** and **10**, bearing a benzylate with pKa of ~15 for the R_1 substituent demonstrated cyclization efficiencies of 40 % and 45 %, respectively (Supplementary Fig. 10). Interestingly, substrates **11** and **12**, which contain a phenolate (pKa of ~10) as the R_1 substituent, exhibited a singular peak corresponding to a peptide with a 6-membered ring in the MALDI spectrum, indicating a cyclization efficiency of 100 % (Fig. 4C and Supplementary Fig. 10). As observed for 5-membered rings, the presence of additional groups (R_2) adjacent to the reaction site does not impede the kinetics of 6-membered ring formation (Supplementary Fig. 13). This demonstrates that substituent choice can be an effective strategy to tune ring formation efficacy, with weaker bases better facilitating the ring formation reaction within the ribosome's active site. This result supports our hypothesis that the weaker phenolate stabilizes the intermediate through more efficient deprotonation, thereby accelerating the rate-limiting step of the cyclization process (Supplementary Fig. 2).

To determine the production yield of the cyclic hydrazinedione product, we used a peptide that exhibited 100 % cyclization efficiency in forming a 6-membered ring. We added an internal standard, a chemically synthesized peptide containing succinic acid (Sa) and **Hz** at the N-terminus of StrepII residues (Sa-**Hz**-WSHPQFEK), at a known concentration to the peptide product. Using the MALDI spectrum (Supplementary Fig. 14), which showed a comparable intensity to the peak of the internal standard, we calculated that ~10 ng of target peptides were produced in 10 μL of the PURExpress™ reaction. Although the yield is low, this result is consistent with the typical production yields of 1–10 ng/μL achievable in the in vitro ribosome-mediated polymerization of ncMs[17].

To further investigate the ribosome's ability to form cyclic structures larger than a 6-membered ring, we tested an additional set of diester substrates with a longer carbon chain than that of succinate diester. Specifically, we synthesized a series of glutarate diester

derivatives (**g**, **g-2**, **16**, and **17**, Supplementary Fig. 3) with the same R_1 substituents and conducted the same procedures for cyclic structure formation (Supplementary Fig. 6). Unfortunately, we were unable to detect a peak corresponding to the theoretical mass of the peptide containing a 7-membered diazepanedione at the N-terminus of a peptide. Instead, only peaks indicating a linear structure were observed in MALDI spectra (Supplementary Fig. 15). This is likely because the rate of the 7-membered ring closure reaction decreases by 1–2 orders of magnitude as the ring size increases from a 5- to 6- to 7-membered ring as observed in solution (Supplementary Fig. 13)[49,50]. In summary, we synthesized 9 distinct pyrazolidinedione and tetrahydropyridazinedione backbones using the rapid ribosomal synthesis.

Cyclization does not occur in solution spontaneously

Our data demonstrate the ribosome's ability to form two distinct cyclic hydrazinedione derivatives (Figs. 2–4). We considered the possibility that these cyclic structures could be formed through an intramolecular self-cyclization reaction in solution, rather than through ribosome-mediated catalysis. To investigate this, we focused on the 6-membered ring produced with substrates **5** and **Hz**, which showed 22 % cyclization efficiency (Fig. 3A). If cyclization were to occur spontaneously in solution, we would expect an increasing proportion of cyclized products over time due to the gradual cyclization of linear products. To verify this, we introduced the purified samples, containing a mixture of 78 % of linear and 22 % of cyclic products, into an aqueous buffer (pH 8.0). The ribosome and target DNA template were omitted to eliminate any potential for producing cyclic products. We monitored the product composition over 24 h through MALDI-TOF mass spectrometry. As shown in Fig. 5A and Supplementary Fig. 16, the ratio of cyclized to linear product remained constant, suggesting that no cyclic products formed by a self-cyclization manner under these conditions (Fig. 5B). We also considered whether additional materials (Strep-Tactin-coated magnetic beads) or chemicals (100 mM Tris-HCl, 150 mM NaCl, 1 mM EDTA, pH 8) used in the experiment might cause a self-cyclization reaction. We used the product obtained from the reaction of **s** and **Hz** and carried out multiple magnetic capture-release experiments to simulate the purification procedure using the same buffer (Supplementary Fig. 17). Not surprisingly, we observed a constant ratio across cycles, further supporting that the observed cyclic structures are not the result of intramolecular self-cyclization during the experiments.

PTC analogues exhibit catalytic activity for cyclization

To directly demonstrate that the cyclic hydrazinedione formation results from the ribosome's catalytic activity, we conducted an additional experiment using functional ribosome analogues that mimic the PTC components of the bacterial 23S ribosomal RNA (Fig. 6A). Specifically, we designed two PTC analogues, P1c2 (70-mer) and P2c (97-mer; Supplementary Information). P1c2 incorporates elements from the P1 region of the ribosome's domain V (Fig. 6B)[51,52], forming a dimer that yields a symmetrical three-dimensional structure similar to the ribosome's active site and is capable of catalyzing peptide bond formation (Fig. 6C). In contrast, P2c is an inactive variant with an extended sequence, despite forming a stable dimeric structure. Using in vitro transcription with T7 RNA polymerase, we synthesized four different PTC analogues ($P1c2^{UGGU}$, P1c2, $P2c^{UGGU}$, and P2c) and $tRNA^{ACCA}$. The 3′-UGGU sequence in the PTC analogues was specifically designed to pair with the complementary 3′-ACCA in tRNA. To assess the functionality of the RNA constructs, we incubated the $P1c2^{UGGU}$ and P1c2 separately and observed that both formed dimeric constructs, regardless of the 3′-UGGU sequence (Supplementary Fig. 18A, B), consistent with previous findings[53]. Additionally, when $P1c2^{UGGU}$ was incubated with $tRNA^{ACCA}$, it produced a construct (Supplementary Fig. 18B), presumably reflecting the formation of a hybridized RNA product via UGGU-ACCA pairing. We hypothesized that this pairing would position the substrates in close proximity for peptide bond formation. Conversely, analogues lacking the complementary UGGU sequence would fail to interact with tRNA, preventing the formation of a cyclic structure.

To test the ribosome's ability to form cyclic structures, we charged substrates **m**, **s**, and **Hz** to $tRNA^{ACCA}$ via Fx, purified them, and mixed **m** with **Hz** and **s** with **Hz** in separate solutions containing the PTC analogues. After the reaction (24 h at 0 °C), we digested the tRNA molecules with RNase (5 min, at room temperature) to isolate and monitor the product attached to the 3′-adenosine residue (Fig. 6C). The crude reaction mixtures were analyzed using liquid chromatography-time-of-flight (LC-TOF) mass spectrometry. The extracted ion chromatogram for the reaction with $P1c2^{UGGU}$ yielded a single peak at 5.0 and 3.3 min corresponding to the mass of the 5- and 6-membered hydrazinedione, respectively (calculated $[M+H]^+$= 422.141, observed $[M+H]^+$= 422.145 in Fig. 6D (blue) and calculated $[M+H]^+$= 436.158, observed $[M+H]^+$= 436.158 in Fig. 6E (blue)). Notably, no peaks corresponding to the 5- or 6-membered rings were observed in the experiments containing P1c2 (Fig. 6D, E (green)). This indicates that the interaction with tRNAs through the UGGU and ACCA sequence is essential for positioning substrates into close proximity and yielding a cyclic structure.

Importantly, the cyclic structure formation could potentially result from the proximity of the substrates on tRNA, rather than the catalytic activity of P1c2. To address this possibility, we performed additional experiments using P2c variants, known to be inactive in peptide bond formation, despite their ability to form a dimeric construct. Consistent with the previous findings[53], we observed that $P2c^{UGGU}$ and P2c formed a dimeric product (Supplementary Fig. 18C), whereas $Pc2^{UGGU}$ produced only a hybridized product with tRNA. However, no peaks corresponding to the masses of 5- or 6-membered rings were detected in samples with the $P2c^{UGGU}$ domain (Fig. 6D, E, purple), strongly suggesting that proximity alone is insufficient to drive peptide and ring formation. Similarly, the Pc2 analog lacking the UGGU sequence also failed to produce the desired products (Fig. 6D, E, orange). These findings indicate that the distinctive sequences of P1c2 and P2c may include key residues required for the catalytic activity in peptide bond formation (see Supplementary Information). Not surprisingly, no peaks corresponding to the 5- and 6-membered cyclic hydrazinedione were detected in the absence of PTC analogues (Fig. 6D, E, black). Utilizing these PTC analogues may provide valuable insights into identifying critical residues for ribosome engineering, potentially enabling the polymerization of a broader range of ncMs.

The reaction products produced in the presence of $P1c2^{UGGU}$ are consistent with the products obtained in the experiments conducted with the full ribosome (Fig. 3C, D). While no linear product was detected in any of the 5-membered hydrazinedione formation reactions of **m** and **Hz**, a linear product was observed in the 6-membered formation reaction of substrate **s** and **Hz** (Supplementary Fig. 19).

Notably, because $P1c2^{UGGU}$ lacks the ability to position substrates sequentially through mRNA codons, a dimeric form of **Hz**-**Hz** linked by a normal peptide bond was observed as a side product. This further confirms the ribosome's catalytic ability to facilitate both cyclic structures and peptide bonds (Supplementary Fig. 20).

Mechanistic proposal for ribosomal synthesis of non-standard ring structure: the α-nitrogen links, and subsequently, the β-nitrogen cyclizes

The ribosome naturally prefers *L*-α-amino acids for peptide bond formation. Several pioneering studies have shown that the ribosome can incorporate β-amino acids[31], albeit with considerably reduced efficiency compared to α-amino acids[9]. This reduced efficiency is presumably due to the extended carbon chain of β-amino acids, which hinders the optimal alignment of the β-nitrogen within the ribosome's peptidyltransferase center for an effective nucleophilic attack on the P-site tRNA. Substrate **Hz**, which has an NH_2 group linked to another

NH_2 group at both the α and β positions, presents unique properties. In reactions involving hydrazine with carboxylic acid derivatives, the β-nitrogen is the primary atom used for bond-forming reactions due to steric hindrance around the α-nitrogen (Fig. 7A)[54]. This raises an important question: can the β-nitrogen outcompete the ribosome's inherent preference for using the α-nitrogen for peptide bond formation within the catalytic site?

The cyclic structures explored in this work have two possible regioisomers. In one scenario, the α-nitrogen atom of the incoming hydrazine ester attacks the ester of the P-site tRNA, while the β-nitrogen targets the ester carbonyl substituted with R_1 (Fig. 7A). Alternatively, the β-nitrogen atom might attack the tRNA linkage, reversing the roles of the nitrogen atoms (Fig. 7B). A critical distinction between these two scenarios is that the first scenario produces a free primary amine in the linear product, while the second scenario does not. This free amine remains reactive, allowing subsequent reactions such as a Schiff base reaction. To identify the regioselectivity involved, we introduced 4-methylbenzaldehyde (4-mba) to the product purified from the PURExpress reaction of **s** and **Hz**, which consists ~80% of the linear product (Fig. 7C, D). Mass spectrometry revealed a single peak, corresponding to the mass of a product containing a hydrazone moiety at the β-nitrogen position (Fig. 7D), suggesting that the α-nitrogen atom attacks the P-site tRNA as shown in Scenario 1 (Fig. 7A). Taken together, these findings confirm that, in ribosome-mediated cyclization, the α-nitrogen atom is used first for linking the nascent peptide chain, and subsequently the β-nitrogen atom undergoes ring closure with the ester carbonyl group substituted with R_1. Despite the lower steric hindrance of the β-nitrogen, the natural ribosome selectively uses the α-nitrogen for peptide bond formation (see Supplementary Fig. 2 for a full proposed mechanism).

Synthesis of non-ribosomal peptide-like products

Direct production of non-ribosomal peptide-like materials may significantly enhance the diversity of peptide drug candidates in a library, particularly when prepared for screening via drug discovery platforms. For example, the RaPID (Random non-standard Peptides Integrated Discovery) system leverages the advantages of diverse cyclic structures, which are crucial for drug efficacy, with template-guided synthesis, inherent to ribosome-based synthesis[40,55]. These molecules are designed to contain multiple cyclic structures, introduced via chemical or enzymatic reactions[56–58], as they enhance thermodynamic stability, resistance to proteolytic degradation, and protein-protein interactions important in therapeutics[32,59–63]. To test the ribosome's ability to directly produce these non-ribosomal peptide-like materials with multiple alternative backbones in a peptide[39], we designed an additional plasmid (pJL1-XZ-StrepII-X'Z) that allows the site-specific incorporation of ncMs (diester and **Hz**) in an alternating manner at the X, Z, X', and Z positions. Additionally, we prepared a diester substrate (**12**) in its amino acid form, enabling the C-terminal incorporation of the diester and producing a cyclic structure with **Hz** incorporated into the next codon within the ribosome. In a separate tube containing PURExpress reaction materials, we supplemented Fx-charged $tRNA^{fMet}$(CAU):**1** and $tRNA^{Pro1E2}$ (GUC):**12**, with $tRNA^{Pro1E2}$ (ACG):**Hz**, respectively, for multiple ring-closing reactions. In the ribosome, **1** and **Hz** incorporated at the **X** and **Z** positions form an N-terminal ring, while **12** and **Hz** at the X' and Z positions form a C-terminal ring. The mass spectra (Fig. 8) yielded peaks of the products containing multiple 5- and 6-membered cyclic backbones, as defined on the mRNA sequence. This suggests the potential for direct synthesis and site-specific incorporation of pharmaceutical cyclic motifs into biopolymers, thereby expanding the range of non-ribosomal peptide-like products in libraries used for peptide drug selection platforms[40].

Discussion

In this work, we demonstrate ribosome-mediated biosynthesis of non-standard cyclic motifs using rationally designed diester and hydrazine substrates (non-canonical monomers, ncMs). These ncMs were charged to tRNA by an acylating-ribozyme then consecutively incorporated into a peptide, with the ribosome catalyzing multiple aminolysis reactions in its catalytic site. Through a series of chemical reactions and mass spectrometric analysis, we revealed that the α-nitrogen atom of the hydrazine monomer extends the monomer onto the nascent peptide chain, while the β-nitrogen undergoes a ring-closing reaction in the ribosome. By varying the length of the

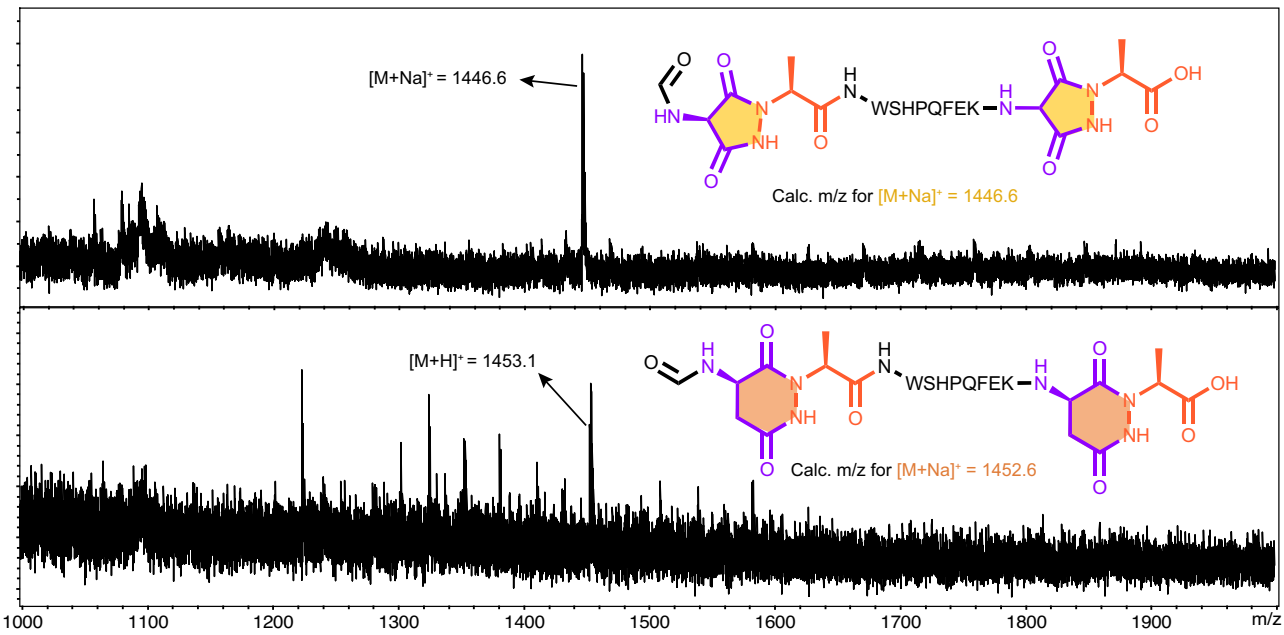

Fig. 8 | MALDI spectrum of the (1)-Hz-StrepII-(1)-Hz and (12)-Hz-StrepII-(12)-Hz peptide. A DNA template engineered to alternately incorporate two ncMs enabled the production of a peptide with multiple cyclic backbone rings. Calculated mass: $[M+H]^+$ = 1423.6 and $[M+H]^+$ = 1452.6 for 5- and 6-membered ring-formation reaction, respectively. The spectra are representative of n = 3 independent experiments. Source data are provided as a Source Data file.

monomer scaffolds, we achieved the formation of diverse 5- and 6-membered cyclic backbones on a peptide. Cyclization efficiencies between 0–100% were observed through rational design of ester substituents.

We believe this breakthrough bridges the gap between the chemical advantages of cyclic motifs in drug-like peptides with the ease of synthesis using the translation machinery, catalyzed by the ribosome. To our knowledge, this study demonstrates the ribosome's capacity to facilitate ring-closing reactions by leveraging the intrinsic biochemical properties of ncMs. Looking ahead, this platform could greatly accelerate the synthesis of heterocyclic motifs. For instance, previous studies using chemical methods showed that incorporating a 5- or 6-membered cyclic hydrazinedione into a peptide required a process of up to seven steps, often under more stringent conditions, such as high temperatures, highly acidic or basic environments[64–66]. In contrast, our approach using the ribosome in vitro produces the same motif in an aqueous buffer within 2 h at 37 °C[67]. This capability could transform the synthesis of the five-membered pyrazolidine motif, already used in small-molecule drugs[68–72]. It could also enhance the production of diverse peptide libraries used for mRNA display-based drug discovery platforms like RaPID[40]. By integrating diverse cyclic structures into the range of peptidomimetics, this approach holds potential to accelerate the development of therapeutic compounds.

Interestingly, the reactions occurring within the ribosome appear to follow conventional chemical principles found in solution. For example, 5-membered ring formation was more efficient than 6- or 7-membered ring formation, and cyclization yield depends on the stability of the leaving group. However, kinetic studies (e.g., entropy, enthalpy, and reaction rates for the ribosome) remain largely unexplored. We expect further kinetic investigations to improve our understanding of the ribosome's catalytic core, enabling the in vitro synthesis of an even greater array of cyclic structures. Admittedly, the product yield in the PURExpress system is low (~10 ng per 10 µL reaction scale, 15-fold lower than the typical yield of peptides composed of the 20 canonical amino acids). However, we anticipate that yields will improve in the future, given that cell-free systems, once limited to µL scales, have now expanded to 200 L scales, with protein yields exceeding grams per liter of reaction[73]. Non-canonical monomer polymerization efficiency could potentially be improved by incorporating an updated set of translational components, such as EF-P, EF-Tu, tRNAs, and ribosomes specially tailored to accommodate ncMs. Future developments in this field may expand the spectrum of possible chemical reactions, potentially transforming our understanding of polymerization chemistry and producing the next generation of medicinal molecules.

Methods

All materials were of the best grade commercially available and used without further purification. NMR solvents (DMSO-d_6) were purchased from Sigma-Aldrich or TCI Chemicals. All the oligonucleotides used in this research were purchased from Integrated DNA Technologies (IDT), Bioneer, or Cosmogenetech and used as received according to manufacturer's guidelines.

General synthesis of substrates

Preparation of diesters. The diester substrates were synthesized in the following ways: (i) We utilized a commercially available molecule containing a carboxylic acid and an ester substituted with R_1 as a starting material or an anhydride that would yield an R_1 ester upon hydrolysis, (ii) Following the formulation of diverse R_1 substituents, we carried out esterification reactions to attach FLG for Fx-charging.

Preparation of hydrazine substrate. The hydrazine substrate was synthesized using a methyl lactate in four steps: (i) replacement of hydroxyl to hydrazino group (triflation on the hydroxyl group followed by attachment of Boc-$NHNH_2$), (ii) conversion of ester to acid by base-catalyzed hydrolysis, (iii) attachment of Boc-ABT, and (iv) Boc deprotection from the β-nitrogen and ABT.

Preparation of activated substrates for flexizyme reaction

General synthetic procedure A. Formation of cyanomethyl ester. To a solution of carboxylic acid (1 eq) triethylamine (0.5 eq) and bromoacetonitrile (10 ml) were added and stirred overnight. After stirring for 16 h at room temperature, the reaction mixture was diluted with EtOAc and washed with HCl (1.0 M in water), $NaHCO_3$ (4 % (w/v) in water), brine, and dried over $MgSO_4$. Brine was used to increase the ionic strength of the aqueous layer, thereby decreasing the solubility of organic compounds in water. The organic phase was concentrated to provide the crude product.

General synthetic procedure B. Formation of dinitrobenzyl esters. To a solution of carboxylic acid (1 eq), 3,5-dinitrobenzyl alcohol (1.2 eq), 4-dimethylaminopyridine (DMAP) (0.5 eq) and *N*-(3-dimethylaminopropyl)-*N*′-ethylcarbodiimide hydrochloride (EDC·HCl) (1.2 eq) were added in dichloromethane. After stirring for 16 h at room temperature, the reaction mixture was diluted with EtOAc and washed with HCl (1.0 M in water), $NaHCO_3$ (4% (w/v) in water), brine, and dried over $MgSO_4$. The organic phase was concentrated to provide the crude product.

General synthetic procedure C. Formation of 4-((2-aminoethyl)carbamoyl)benzyl thioates. To a solution of carboxylic acid (1.0 eq), *tert*-butyl 2-[4-(mercaptomethyl)benzamido]ethyl carbamate (Boc-ABT) (0.3 eq), 4-dimethylaminopyridine (DMAP) (0.5 eq) and *N*-(3-dimethylaminopropyl)-*N*′-ethylcarbodiimide hydrochloride (EDC·HCl) (1.0 eq) were added in DCM. After stirring for 16 h at room temperature, the reaction mixture was diluted with EtOAc and washed with HCl (1.0 M in water), $NaHCO_3$ (4% (w/v) in water), brine, and dried over $MgSO_4$. The organic phase was concentrated to provide the crude product.

General Fx-mediated acylation reaction

Microhelix acylation. A reaction mixture was prepared in a PCR tube by combining 1 µL of 0.5 M HEPES (pH 7.5) or bicine (pH 8.8), 1 µL of 10 µM microhelix, 1 µL of 10 µM eFx, dFx, or aFx, and 3 µL of nuclease-free water. The solution was heated to 95 °C for 2 min and then allowed to cool to room temperature over 5 min. After cooling, 2 µL of 300 mM $MgCl_2$ was added, and the mixture was incubated at room temperature for 5 min. The reaction was subsequently chilled on ice for 2 min, followed by the addition of 2 µL of 10–50 mM activated-ester substrate in DMSO. The final mixture was incubated at 0 °C for 16–120 h.

tRNA acylation. In a separate PCR tube, 2 µL of 0.5 M HEPES (pH 7.5) or bicine (pH 8.8), 2 µL of 250 µM tRNA, 2 µL of 250 µM Fx (selected from the microhelix screen), and 3 µL of nuclease-free water were combined. The mixture was heated to 95 °C for 2 min and allowed to cool to room temperature over 5 min. After cooling, 4 µL of 300 mM $MgCl_2$ was added, and the solution was incubated at room temperature for 5 min. The reaction was then chilled on ice for 2 min, followed by the addition of 4 µL of 10–50 mM activated-ester substrate in DMSO. The final mixture was incubated on ice at 0 °C for 16–120 h.

In vitro synthesis of cyclic hydrazinediones

Ribosome-mediated synthesis of cyclic hydrazinediones. As a reporter peptide, a T7 promoter-controlled DNA template (pJL1_XZ-StrepII) was designed to encode a streptavidin (Strep) tag and additional Met(AUG) and Ile(AUC) codons (XZWSHPQFEKST (strep-tag), where X and Z indicate the position of the diester and Hz substrates, respectively) for N-terminal incorporation of two ncMs. The synthesis was performed using only the 9 amino acids that decode the purification tag without the other 11 amino acids to prevent corresponding

endogenous tRNAs from being aminoacylated and participating in translation. The PURExpress™ Δ (aa, tRNA) kit (NEB, E6840S) was used for in vitro ribosomal synthesis and the reaction mixtures were incubated at 37 °C for 2 h. The synthesized peptides were then purified using Strep-Tactin®-coated magnetic beads (IBA), denatured with a 0.1 % (v/v) SDS solution in water, and characterized by MALDI-TOF mass spectrometry.

Multiple syntheses of cyclic hydrazinediones. A plasmid (pJL1-XZ-StrepII-X′Z) encoding the XZWSHPQFEKSX′Z was used for multiple ring-closing reactions, where X, X′, and Z indicate the position of the diester (**1**, **12**) and **Hz**, respectively. The diesters were incorporated into the Met (AUG-X) and Asp (GAC-X′) codons. Simultaneously, **Hz** was incorporated into the Arg (CGU-Z) codon. The reaction mixtures, containing only the 8 amino acids necessary for decoding the Strep tag, were incubated at 37 °C for 2 h. The reaction mixtures were incubated at 37 °C for 2 h. The resulting products were purified and characterized by the same method described below.

Purification and characterization of cyclic hydrazinediones

The products containing hydrazinediones were purified using an affinity tag purification technique or a C18 spin column purification. The purified products were characterized by MALDI spectrometry. For MALDI sample preparation, the purified peptide in 1.5 μL of SDS solution was dried with 0.5 μL of the matrix (α-cyano-4-hydroxycinnamic acid in THF, 10 mg·mL^{-1}). The dried sample was characterized on a Bruker Autoflex MALDI-TOF and processed using Compass DataAnalysis (Bruker).

Reaction of hydrazone between hydrazine and aldehyde

The sample was freeze-dried to remove a solvent (water). Then, the solid-state peptide was dissolved by 4-methylbenzaldehyde (TCI, T0259) and incubated for 30 min at 37 °C. Afterward, water was added again, and if layer separation occurs, the upper aqueous layer was characterized by MALDI-TOF and processed using Compass DataAnalysis (Bruker).

Formation of cyclic hydrazinedione using PTC analogues (P1c2^{UGGU}, P1c2, P2c^{UGGU}, and P2c)

1,000 pmol of PTC analogues was separately dissolved in 32 μL of 62.5 mM HEPES (pH 7.5). To the cooled mixture, 8 μL of 300 mM $MgCl_2$ was added, and incubated on ice for 60 min to allow self-dimerization. Then, 1,000 pmol of tRNA^{fMet} (CAU):**s** and tRNA^{fMet} (CAU):**Hz** was added and placed at 0 °C for 24 h for cyclic hydrazinedione formation reaction. After the reaction, each product was treated with 44 μL RNase A solution (RNase A (Favorgen) and 200 mM sodium acetate, pH 5.2) to liberate any cyclic hydrazinedione that may have formed from tRNA, and incubated at room temperature for 5 min. The RNase-treated samples were directly used for LC–MS analysis without further purification process.

Statistics and reproducibility

No statistical methods were used to predetermine sample size, and no samples were excluded from the analysis. The experiments were not randomized, and investigators were not blinded.

Reporting summary

Further information on research design is available in the Nature Portfolio Reporting Summary linked to this article.

Data availability

The ribosome model shown in Fig. 1, Fig. 6, and Supplementary Fig. 2 was rendered from Protein Data Bank entry 1VY4 (*E. coli* 70S ribosome bound to a peptidyl-tRNA mimic; [https://www.rcsb.org/structure/1VY4]). All characterization data (NMR spectroscopy and mass spectrometry) are provided within the Article and its Supplementary Information. The full source dataset has been archived on Zenodo and is available at [https://doi.org/10.5281/zenodo.15304159]. Source data are provided with this paper.

References

1. Sievers, A., Beringer, M., Rodnina, M. V. & Wolfenden, R. The ribosome as an entropy trap. *Proc. Natl. Acad. Sci. USA* **101**, 7897–7901 (2004).
2. Rodnina, M. V., Beringer, M. & Bieling, P. Ten remarks on peptide bond formation on the ribosome. *Biochem. Soc. Trans.* **33**, 493–498 (2005).
3. Bieling, P., Beringer, M., Adio, S. & Rodnina, M. V. Peptide bond formation does not involve acid-base catalysis by ribosomal residues. *Nat. Struct. Mol. Biol.* **13**, 423–428 (2006).
4. Li, G.-W., Oh, E. & Weissman, J. S. The anti-Shine–Dalgarno sequence drives translational pausing and codon choice in bacteria. *Nature* **484**, 538–541 (2012).
5. Krayevsky, A. A. & Kukhanova, M. K. The peptidyltransferase center of ribosomes. *Prog. Nucleic Acid Res. Mol. Biol.* **23**, 1–51 (1979).
6. Nierhaus, K., Schulze, H. & Cooperman, B. Molecular mechanisms of the ribosomal peptidyltransferase center. *Biochem. Int.* **1**, 185–192 (1980).
7. Rogers, J. M. & Suga, H. Discovering functional, non-proteinogenic amino acid containing, peptides using genetic code reprogramming. *Org. Biomol. Chem.* **13**, 9353–9363 (2015).
8. Katoh, T. & Suga, H. Ribosomal incorporation of consecutive beta-amino acids. *J. Am. Chem. Soc.* **140**, 12159–12167 (2018).
9. Lee, J. et al. Ribosomal incorporation of cyclic β-amino acids into peptides using in vitro translation. *Chem. Commun.* **56**, 5597–5600 (2020).
10. Ohshiro, Y. et al. Ribosomal synthesis of backbone-macrocyclic peptides containing gamma-amino acids. *Chembiochem* **12**, 1183–1187 (2011).
11. Tsiamantas, C. et al. Ribosomal incorporation of aromatic oligoamides as peptide sidechain appendages. *Angew. Chem. Int Ed. Engl.* **59**, 4860–4864 (2020).
12. Katoh, T. & Suga, H. Ribosomal elongation of cyclic gamma-amino acids using a reprogrammed genetic code. *J. Am. Chem. Soc.* **142**, 4965–4969 (2020).
13. Goto, Y., Murakami, H. & Suga, H. Initiating translation with D-amino acids. *RNA* **14**, 1390–1398 (2008).
14. Katoh, T., Tajima, K. & Suga, H. Consecutive elongation of D-amino acids in translation. *Cell Chem. Biol.* **24**, 46–54 (2017).
15. Kawakami, T., Ishizawa, T. & Murakami, H. Extensive reprogramming of the genetic code for genetically encoded synthesis of highly N-alkylated polycyclic peptidomimetics. *J. Am. Chem. Soc.* **135**, 12297–12304 (2013).
16. Goto, Y., Katoh, T. & Suga, H. Flexizymes for genetic code reprogramming. *Nat. Protoc.* **6**, 779–790 (2011).
17. Lee, J. et al. Ribosome-mediated biosynthesis of pyridazinone oligomers in vitro. *Nat. Commun.* **13**, 6322 (2022).
18. Ugwumba, I. N. et al. Improving a natural enzyme activity through incorporation of unnatural amino acids. *J. Am. Chem. Soc.* **133**, 326–333 (2011).
19. Agostini, F. et al. Biocatalysis with unnatural amino acids: enzymology meets xenobiology. *Angew. Chem. Int Ed. Engl.* **56**, 9680–9703 (2017).
20. Drienovská, I. & Roelfes, G. Expanding the enzyme universe with genetically encoded unnatural amino acids. *Nat. Catal.* **3**, 193–202 (2020).
21. Burke, A. J. et al. Design and evolution of an enzyme with a non-canonical organocatalytic mechanism. *Nature* **570**, 219–223 (2019).

22. Axup, J. Y. et al. Synthesis of site-specific antibody-drug conjugates using unnatural amino acids. *Proc. Natl. Acad. Sci. USA* **109**, 16101–16106 (2012).
23. Tsuchikama, K., Anami, Y., Ha, S. Y. Y. & Yamazaki, C. M. Exploring the next generation of antibody-drug conjugates. *Nat. Rev. Clin. Oncol.* **21**, 203–223 (2024).
24. Schlippe, Y. V., Hartman, M. C., Josephson, K. & Szostak, J. W. In vitro selection of highly modified cyclic peptides that act as tight binding inhibitors. *J. Am. Chem. Soc.* **134**, 10469–10477 (2012).
25. Wang, L. et al. Therapeutic peptides: current applications and future directions. *Signal Transduct. Target Ther.* **7**, 48 (2022).
26. Alavi, S. E., Cabot, P. J. & Moyle, P. M. Glucagon-like peptide-1 receptor agonists and strategies to improve their efficiency. *Mol. Pharm.* **16**, 2278–2295 (2019).
27. Josephson, K., Ricardo, A. & Szostak, J. W. mRNA display: from basic principles to macrocycle drug discovery. *Drug Discov. Today* **19**, 388–399 (2014).
28. Passioura, T., Katoh, T., Goto, Y. & Suga, H. Selection-based discovery of druglike macrocyclic peptides. *Annu Rev. Biochem* **83**, 727–752 (2014).
29. Ohta, A., Murakami, H. & Suga, H. Polymerization of alpha-hydroxy acids by ribosomes. *Chembiochem* **9**, 2773–2778 (2008).
30. Maini, R. et al. Ribosomal formation of thioamide bonds in polypeptide synthesis. *J. Am. Chem. Soc.* **141**, 20004–20008 (2019).
31. Katoh, T. & Suga, H. Consecutive ribosomal incorporation of alpha-aminoxy/alpha-hydrazino acids with l/d-configurations into nascent peptide chains. *J. Am. Chem. Soc.* **143**, 18844–18848 (2021).
32. Hill, T. A., Shepherd, N. E., Diness, F. & Fairlie, D. P. Constraining cyclic peptides to mimic protein structure motifs. *Angew. Chem. Int Ed. Engl.* **53**, 13020–13041 (2014).
33. Malde, A. K., Hill, T. A., Iyer, A. & Fairlie, D. P. Crystal structures of protein-bound cyclic peptides. *Chem. Rev.* **119**, 9861–9914 (2019).
34. Goto, Y., Ito, Y., Kato, Y., Tsunoda, S. & Suga, H. One-pot synthesis of azoline-containing peptides in a cell-free translation system integrated with a posttranslational cyclodehydratase. *Chem. Biol.* **21**, 766–774 (2014).
35. Goto, Y. & Suga, H. In vitro biosynthesis of peptides containing exotic azoline analogues. *Chembiochem* **21**, 84–87 (2020).
36. Grasso, K. T. et al. Structural robustness affects the engineerability of aminoacyl-tRNA synthetases for genetic code expansion. *Biochemistry* **60**, 489–493 (2021).
37. Lee, J. et al. Expanding the limits of the second genetic code with ribozymes. *Nat. Commun.* **10**, 5097 (2019).
38. Niwa, N., Yamagishi, Y., Murakami, H. & Suga, H. A flexizyme that selectively charges amino acids activated by a water-friendly leaving group. *Bioorg. Med Chem. Lett.* **19**, 3892–3894 (2009).
39. Choi, Y. N. et al. Programmable synthesis of biobased materials using cell-free systems. *Adv. Mater.* **35**, e2203433 (2023).
40. Goto, Y. & Suga, H. The RaPID platform for the discovery of pseudo-natural macrocyclic peptides. *Acc. Chem. Res* **54**, 3604–3617 (2021).
41. Jones R. G. Reactions of Hydrazine with Heterocyclic 1,2-Dicarboxylic Acid Esters. *Am. Chem. Soc.* **78**, 159–163 (1956).
42. Kang, C. W., Ranatunga, S., Sarnowski, M. P. & Del Valle, J. R. Solid-phase synthesis of tetrahydropyridazinedione-constrained peptides. *Org. Lett.* **16**, 5434–5437 (2014).
43. Robertson, W. E. et al. Sense codon reassignment enables viral resistance and encoded polymer synthesis. *Science* **372**, 1057–1062 (2021).
44. McClelland, R. A. Rate-limiting deprotonation in tetrahedral intermediate breakdown. *J. Am. Chem. Soc.* **106**, 7579–7583 (1984).
45. Bender, M. L. Mechanisms of catalysis of nucleophilic reactions of carboxylic acid derivatives. *Chem. Rev.* **60**, 53–113 (1960).
46. Schmidt, T. G. M. & Skerra, A. The Strep-tag system for one-step purification and high-affinity detection or capturing of proteins. *Nat. Protoc.* **2**, 1528–1535 (2007).
47. Imanishi, S. et al. In vitro selection of macrocyclic d/l-hybrid peptides against human EGFR. *J. Am. Chem. Soc.* **143**, 5680–5684 (2021).
48. Iwane, Y., Kimura, H., Katoh, T. & Suga, H. Uniform affinity-tuning of N-methyl-aminoacyl-tRNAs to EF-Tu enhances their multiple incorporation. *Nucleic Acids Res.* **49**, 10807–10817 (2021).
49. Baldwin J. Rules for ring closure. *Ciba Found Symp*. 85–99 (1978).
50. Illuminati, G., Mandolini, L. & Masci, B. Ring-closure reactions. V. Kinetics of five- to ten-membered ring formation from o-.omega.-bromoalkylphenoxides. Influence of the O-heteroatom. *J. Am. Chem. Soc.* **97**, 4960–4966 (1975).
51. Kawabata M. et al. Peptide bond Formation between aminoacyl-minihelices by a scaffold derived from the peptidyl transferase center. *Life (Basel)* **12**, 573 (2022).
52. Agmon I. On the Re-Creation of Protoribosome Analogues in the Lab. *Int. J. Mol. Sci.* **25**, 4960 (2024).
53. Bose, T. et al. Origin of life: protoribosome forms peptide bonds and links RNA and protein dominated worlds. *Nucleic Acids Res.* **50**, 1815–1828 (2022).
54. Schmidt E. W. *Hydrazine and Its Derivatives: Preparation, Properties, Applications, 2 Volume Set* 2nd edn (John Wiley & Sons, 2001).
55. Passioura, T. & Suga, H. A RaPID way to discover nonstandard macrocyclic peptide modulators of drug targets. *Chem. Commun. (Camb.)* **53**, 1931–1940 (2017).
56. Ozaki, T. et al. Dissection of goadsporin biosynthesis by in vitro reconstitution leading to designer analogues expressed in vivo. *Nat. Commun.* **8**, 14207 (2017).
57. Fleming, S. R. et al. Flexizyme-enabled benchtop biosynthesis of thiopeptides. *J. Am. Chem. Soc.* **141**, 758–762 (2019).
58. Tsutsumi, H., Kuroda, T., Kimura, H., Goto, Y. & Suga, H. Post-translational chemical installation of azoles into translated peptides. *Nat. Commun.* **12**, 696 (2021).
59. Le Bourdonnec, B. et al. Synthesis and pharmacological evaluation of new pyrazolidine-3,5-diones as AT1 angiotensin II receptor antagonists. *J. Med. Chem.* **43**, 2685–2697 (2000).
60. Dick, M. et al. Pyrazolidine-3,5-dione-based inhibitors of phosphoenolpyruvate carboxylase as a new class of potential C(4) plant herbicides. *FEBS Lett.* **591**, 3369–3377 (2017).
61. Corbi-Verge, C., Garton, M., Nim, S. & Kim, P. M. Strategies to develop inhibitors of motif-mediated protein-protein interactions as drug leads. *Annu Rev. Pharm. Toxicol.* **57**, 39–60 (2017).
62. Checco, J. W. et al. alpha/beta-peptide foldamers targeting intracellular protein-protein interactions with activity in living cells. *J. Am. Chem. Soc.* **137**, 11365–11375 (2015).
63. Vinogradov, A. A. et al. A compact reprogrammed genetic code for de novo discovery of proteolytically stable thiopeptides. *J. Am. Chem. Soc.* **146**, 8058–8070 (2024).
64. Zhang, X.-Y. et al. Synthesis, in vitro and in vivo anticancer activities of novel 4-substituted 1, 2-bis (4-chlorophenyl)-pyrazolidine-3, 5-dione derivatives. *MedChemComm* **6**, 1781–1786 (2015).
65. Kumar, H. & Jain, S. Synthesis and antimicrobial evaluation of 4-benzylidene-pyrazolidine-3, 5-dione derivatives. *Int. J. Pharm. Sci. Res.* **4**, 453 (2013).
66. Nadipour, F., Salahvarzi, S. & Dadgar, Z. Investigating the synthesis methods of 3, 5-dione pyrazolidine and 3, 5-dione 1-phenylpyrazolidine in the presence and absence of ultrasound bath and their anticancer effects on MCF-7 breast cancer cells. *Curr. Bioact. Compd.* **20**, 51–56 (2024).
67. Miura, T., Lee, K. J., Katoh, T. & Suga, H. In vitro selection of macrocyclic l-α/d-α/β/γ-hybrid peptides targeting IFN-γ/IFNGR1 protein–protein interaction. *J. Am. Chem. Soc.* **146**, 17691–17699 (2024).

68. He, Z. X., Gong, Y. P., Zhang, X., Ma, L. Y. & Zhao, W. Pyridazine as a privileged structure: an updated review on anticancer activity of pyridazine containing bioactive molecules. *Eur. J. Med Chem.* **209**, 112946 (2021).
69. Yang, Y. et al. 3,5-dioxopyrazolidines, novel inhibitors of UDP-N-acetylenolpyruvylglucosamine reductase (MurB) with activity against gram-positive bacteria. *Antimicrob. Agents Chemother.* **50**, 556–564 (2006).
70. Macbeth, R. A. & Fischer, J. D. The effect of oral oxyphenbutazone (Tandearil) on tumor growth and the level of the seromucoid fraction in rats bearing walker 256 carcinoma. *Can. J. Physiol. Pharm.* **49**, 1071–1077 (1971).
71. Kapadia, G. J. et al. Inhibition of epstein-barr virus early antigen activation promoted by 12-O-tetradecanoylphorbol-13-acetate by the non-steroidal anti-inflammatory drugs. *Cancer Lett.* **161**, 221–229 (2000).
72. Heimark, L. D. et al. The effect of sulfinpyrazone on the disposition of pseudoracemic phenprocoumon in humans. *Clin. Pharm. Ther.* **42**, 312–319 (1987).
73. Zawada, J. F. et al. Microscale to manufacturing scale-up of cell-free cytokine production-a new approach for shortening protein production development timelines. *Biotechnol. Bioeng.* **108**, 1570–1578 (2011).
74. Katoh, T. & Suga, H. Drop-off-reinitiation at the amino termini of nascent peptides and its regulation by IF3, EF-G, and RRF. *RNA* **29**, 663–674 (2023).
75. Katoh, T. & Suga, H. Translation initiation with exotic amino acids using EF-P-responsive artificial initiator tRNA. *Nucleic Acids Res* **51**, 8169–8180 (2023).
76. Goto, Y. & Suga, H. Translation initiation with initiator tRNA charged with exotic peptides. *J. Am. Chem. Soc.* **131**, 5040–5041 (2009).
77. Tharp, J. M. et al. Initiation of protein synthesis with non-canonical amino acids in Vivo. *Angew. Chem. Int Ed. Engl.* **59**, 3122–3126 (2020).

Acknowledgements

This research was supported by the National Research Foundation (NRF) funded by the Korea government (MSIT): NRF-2021R1C1C1006129, RS-2025-00520898, and Bio&Medical Technology Development Program, RS-2024-00400486.

Author contributions

KL, HP, and JL planned the research and designed the experiments. KL and HP carried out synthesis of substrates, acylation reactions of substrates, in vitro oligomerization reactions, and mass spectrometric characterization. HP and RKD carried out synthesis of substrates. DI and JS performed mass-spectrometric analysis. All authors wrote the manuscript. JL supervised this study.

Competing interests

The authors declare no competing interests.

Additional information

Supplementary information The online version contains supplementary material available at https://doi.org/10.1038/s41467-025-60126-4.

Correspondence and requests for materials should be addressed to Joongoo Lee.

Peer review information *Nature Communications* thanks the anonymous reviewers for their contribution to the peer review of this work. A peer review file is available.